Characterization of surface crack depth and repair evaluation using Rayleigh waves

D. G. Aggelis[a,b], T. Shiotani[c], D. Polyzos[d*]

[a]*Research Institute of Technology, Tobishima Corporation, 5472 Kimagase, Noda, Chiba, 270-0222, Japan*

[b]*Department of Materials Science and Engineering, University of Ioannina, 45110 Ioannina, Greece*

[c]*Graduate School of Engineering, Kyoto University, C1-2-236, Katsura, Kyoto, 615-8540, Japan*

[d]*Mechanical Engineering and Aeronautics Dept., University of Patras, P.O. Box 1401, Rion 26504, Greece*

Abstract. The issues of surface crack depth determination and the evaluation of repair effectiveness are not trivial for concrete engineers. In the present paper, surface waves are applied on concrete blocks with artificial slots to correlate wave parameters with crack depth. The repair of cracks in situ by the use of injection material is simulated by applying epoxy in slots in laboratory and quantification of the filling percentage is attempted. Simultaneously, a frequency domain Boundary Element Method is employed for the numerical simulation of transient pulses interacting with surface breaking cracks. Experimental results compare well with numerical, showing that the repair effectiveness, which so far can be evaluated only by destructive techniques, is possible by simple surface wave measurements.

Keywords: Characterization, cracks, epoxy, repair, surface waves.

[*] Corresponding author. *Tel: +30 2610 997236, Fax: +30 2610 997234. E-mail address: polyzos@mech.upatras.gr*

1. Introduction

Surface cracks are the most common kind of defects in concrete structures. Some of the reasons are overloading, weathering, drying shrinkage, differential settlement, other degradation processes or combination of the above. The major threat they pose concerns the exposure of the metal reinforcement to environmental agents leading to its oxidation [1-5]. In order to seal the crack sides and protect the interior, providing also structural strength restoration, injection of epoxy or other agent can be used [6-8]. However, both the evaluation of the repair efficiency, as well as the determination of the initial crack depth, are not trivial tasks.

Ultrasonic waves have been used as a non destructive technique in the case of crack characterization. The transit time of longitudinal waves diffracted by the tip of the crack can be used for the estimation of crack depth [9,10]. However, the cracks in concrete are in many cases filled with water or dust. Additionally, the surfaces of a crack in reinforced concrete may also be in contact at isolated spots. The contact faces, filling or steel bars can carry the compressional wave. Therefore, when a crack reaches large depth, it is possible that the energy carried through the tip of the crack is similar or lower than the energy carried by the bridging points. Under such circumstances the short-path wave could be mistaken for the wave expected by the tip, and the crack would be underestimated [10-12]. Therefore, the use of Rayleigh waves has been studied extensively as an alternative [1,13-15].

Rayleigh waves are constrained near the surface of the material, while their energy propagates mainly up to thickness equal to one wavelength. Their advantage is that they

carry higher amount of energy than bulk waves, as well as their lower geometric spreading, that allows them to propagate at longer distances [16]. In many of the above cited studies and others [17-26], amplitude or energy related parameters, as well as frequency content has been related to artificial cracks' parameters for different materials.

One of the aims of this study is to contribute to a methodology for surface crack characterization in concrete that is not established so far. Another crucial issue that has not received proper attention is the evaluation of the repair after epoxy injection. Specifically, even if the amount of the injected agent is known, still the percentage of filling of the empty crack volume cannot be estimated because the internal pattern of the crack is not known. To this end, surface wave propagation is useful, since the epoxy layer provides an additional path for the wave, influencing the amplitude and other transmission parameters.

Herein, the correlation of wave parameters with the depth of artificially machined slots in concrete prism specimens is studied. The wave amplitude exhibits a decreasing trend with the slot depth, as expected. Additionally, complete filling of some slots with epoxy showed that the waveform energy is comparable to the case of healthy material, while the partial filling of the slot is also examined. Some experimental results of the preliminary phase of this study can be found in [27]. As an actual example, the examination of surface opening cracks on a concrete bridge deck before and after repair with epoxy is indicatively described, showing that after successful application of epoxy and sealing of the crack, the Rayleigh propagation is restored to the level of sound concrete.

Simultaneously, numerical simulations were performed using a Boundary Element Method code. The code utilizes the transformation of the signal to frequency domain in order to decompose the problem to a sequence of boundary value problems [28]. The final waveform is reached by the inversion of the solution back to time domain. A parametric study was conducted to examine the propagation of different frequencies through several slots. The results show the trend of amplitude reduction with the slot depth, while the filling of the slot with material of inferior elastic properties (like epoxy) seems to restore the propagation to the level of the sound material, supporting the experimental results. Also, the comparison between the numerical and experimental results leads to interesting conclusions about the actual penetration depth of Rayleigh waves in concrete.

2. Experimental details

2.1 Materials

Two concrete specimens were cast using water to cement ratio of 0.43 and maximum aggregate size of 20 mm. The specimens were of prism shape (150x150x500 mm). After the completion of curing (28 days in water), eight slots of different depths were machined, specifically 2, 4, 7, 8.5, 9.5, 13.5, 19 and 23 mm, perpendicular to the longitudinal axis of the specimen. Two slots were cut on opposite surfaces of each specimen with a sufficient distance of at least 150 mm between them to avoid interactions. The slot width was 4 mm. For the 2 mm slot, it is obvious that the depth was less than the width. This makes it an unusual case but it was inevitable due to the machining wheel. In any case it still reduces the

effective cross section of the specimen, blocking a part of the energy, which is reflected on the reduced amplitude of the transmitted wave.

The epoxy used for filling of the cracks in order to simulate the repair process, was a two component epoxy adhesive, suitable for concrete. Its density is 1100 kg/m^3, the set time is 5 min and sufficient hardening is obtained in 1 hr at 20 ^{o}C. Measurements were conducted after 1 day, when nominally the epoxy exhibits strength of 12 MPa and elastic modulus of 1 GPa.

2.2 Sensors and excitation

Although different configurations were tested, results from pulse generator C-101-HV of Physical Acoustics Corp, PAC, with a main excitation frequency of around 115 kHz, and the 1910 function synthesizer of NF Electronic Instruments are discussed. Concrete, due to attenuation, limits the propagating frequencies to bands around or below 100 kHz. Therefore, sensitive sensors at this range were used, namely R6, PAC. However, measurements with broadband sensors, i.e. Fujiceramics FC 1045S, were also conducted to confirm that the resulting trends were not dependent on the sensors' frequency response. The representation of the experimental setup can be seen in Fig. 1. In order to choose a suitable pulser-receiver separation, different distances were tested in sound material. A separation of 60 mm was chosen to avoid near field effects. The second receiver was placed 40 mm away from the first with the slot in the middle between the sensors, see Fig. 1. After all sensors (transducer and two receivers) were placed on the specimen, the pulse generator was triggered manually to generate an electric pulse. This was directed to the transducer which transformed it into stress wave and transmitted it into the material. This pulse gives rise to all kinds of waves;

longitudinal, shear (spreading into the specimen with a spherical wavefront) and Rayleigh which are confined near the surface (see Fig. 1). The receivers can record the Rayleigh mode which is the strongest but also the initial part of longitudinal which is the fastest type and therefore its contribution arrives first. According to the slot depth, the amplitude of the Rayleigh wave propagating through will be reduced. The reduction of this amplitude relatively to the slot depth is of major interest for the scope of this study. It is noted that a thin layer of grease was applied between the sensors and the specimen surface to ensure acoustical coupling. The excitation was conducted from both sides, resulting in similar trends. Although this study focuses on energy parameters, the use of two sensors is essential for velocity measurements, as well as reliability issues.

3. Boundary Element Method simulation

The method employed herein has been successfully used for the theoretical treatment of scattering problems [28]. Therefore, in this section, the BEM machinery used for the solution of the two dimensional Rayleigh wave-crack interaction problems will be explained in brief. Consider a two-dimensional linear elastic half-space (similar to Fig. 1) of surface S, part of which, belongs to a surface breaking crack located in a distance ℓ from the external transient displacement excitation, as it is depicted in Fig. 1. Applying the Fast Fourier Transform (FFT) on the signal the just described time domain problem is decomposed to a sequence of harmonic boundary value problems each of which is solved via the BEM methodology explained below. In order to minimize the aliasing phenomena the exponential window method proposed by Kausel and Röesset [29] is utilized, where complex frequencies with a

small imaginary part of the form: $\omega_c = \omega - jc$ are used. The constant c is set equal to $0.65\Delta\omega$ where $\Delta\omega$ is the frequency step used in FFT. After solving numerically the problem in the frequency domain and then applying the inverse Fourier transform, the time response is rescaled with the aid of the exponential factor e^{ct}.

For each frequency ω, the developed displacement **u** satisfies the Navier–Cauchy differential equation:

$$\mu\nabla^2\mathbf{u} + (\lambda+\mu)\nabla\nabla\cdot\mathbf{u} + \rho\omega^2\mathbf{u} = \mathbf{0} \tag{1}$$

where λ, μ and ρ stand for the Lame constants and the mass density, respectively, ∇ is the gradient operator and ω the excitation frequency. Considering an infinite elastic space, the fundamental displacement tensor $\mathbf{u}^*$ of the above differential equation [28] and employing the well-known Betti's reciprocal identity, one can obtain the integral representation of the above described harmonic problem, written in the form

$$a\mathbf{u}(\mathbf{x}) + \int_{S-S_1-S_2} \mathbf{t}^*(\mathbf{x},\mathbf{y},\omega)\cdot\mathbf{u}(\mathbf{y})dS_\mathbf{y} + \int_{S_1} \mathbf{t}^*(\mathbf{x},\mathbf{y},\omega)\cdot\mathbf{u}(\mathbf{y})dS_\mathbf{y} = \\ = \int_{S_2} \mathbf{t}^*(\mathbf{x},\mathbf{y},\omega)\cdot\mathbf{U}(\mathbf{y},\omega)dS_\mathbf{y} \tag{2}$$

with x being the point where the corresponding displacement vector **u** is evaluated, $\mathbf{t}^*$ is the traction tensor corresponding to the fundamental solution $\mathbf{u}^*$ and **U** is the excitation displacement vector corresponding to frequency ω. The surface S_1 represents the free surface of the slot, S_2 the surface where the excitation is taken place and S-S_1-S_2 the rest

infinite free surface of the considered half space. The coefficient α obtains the value 1 for internal to the concrete points and the value 1/2 when boundary points are considered.

In order to solve numerically Eq. (2) in the framework of the BEM presented in [28], S_1, S_2 and part of the free half-space surface S are discretized into isoparametric quadratic line elements. For smooth boundaries full continuous elements are employed, while a combination of continuous–discontinuous or partially discontinuous elements are used in order to treat boundaries with corners and discontinuous boundary conditions. The truncation of the free surface S is accomplished by considering that the reflected Rayleigh waves do not affect the transient signal at the observation point [30]. In all problems solved here and for all the considered excitations, high convergence is achieved by using four isoparametric quadratic elements per the wave-length corresponding to the central frequency of the FFT spectrum of the incident pulse.

Collocating the discretized integral Eq. (2) at each node, one obtains a system of linear algebraic equations having the form

$$[\mathbf{H}]\cdot\{\mathbf{u}\}=\{\mathbf{b}\} \tag{3}$$

where the vectors $\{\mathbf{u}\},\{\mathbf{b}\}$ contain all the unknown and known nodal displacement components, respectively, and [H] is a matrix with complex elements each of which is a function of frequency, material properties and structure's geometry. The diagonal elements of [H] are strongly singular integrals evaluated with the aid of an advanced direct integration technique proposed by Guiggiani and Casalini [31]. The linear algebraic system (3) is solved

numerically through a LU decomposition algorithm and the evaluated displacements are converted to time domain through the inverse FFT procedure proposed in [29].

Finally for the cases of partially and fully filled slots, one more integral equation corresponding to the region of resin is considered. At the resin-concrete interfaces continuity conditions on displacements and tractions are applied.

4. Results

4.1 Relation of amplitude to slot depth

In Fig. 2(a) some indicative waveforms are presented concerning the case of empty slot measured with the excitation of 115 kHz and the resonance transducers. Taking into account the measured Rayleigh velocity of the specific material (2400 m/s), the major wavelength is calculated at 21 mm (ratio of velocity to frequency). The waveforms are recorded by the second receiver (see Fig. 1), namely 100 mm from the excitation. In the first waveform of Fig. 2(a) sound material, it is clear that after the initial longitudinal arrivals, a strong Rayleigh burst is observed [9,32]. The existence of the slots certainly decreases the amplitude of the wave, as seen for the cases of 2 mm, 9.5 mm and 13.5 mm depth, see again the waveforms of Fig. 2(a).

In Fig. 2(b) one can see the results of the numerical analysis for the corresponding problem. Also in this case, the longitudinal arrivals are seen before the strong Rayleigh burst. The

amplitude of the waveforms certainly decreases with the slot depth, even between the last two cases of larger slots, something that was not clear for the experimental results. This trend will be studied throughout this paper. It is mentioned that the duration of the experimental signals in Fig. 2(a) is long due to the sensitivity of the resonant sensors that exhibit the so called "ringing" behavior.

In Fig. 3(a), the relation between waveform amplitude measured by the second transducer (normalized by the amplitude on sound material) and slot depth is depicted for numerical and experimental results. They both follow a curve of exponential decay. However, it is actually seen that the amplitude of experimental waveforms, ceases to be sensitive to the depth for large slots and seems to converge to a value around 0.3. On the other hand, the computed amplitude decreases in a more steep way, while at the slot of 23 mm, it is almost zero.

4.2 Use of longer wavelength

In many cases, the slot depth is divided by the major wavelength in order to provide a dimensionless relationship that hopefully holds for any scale [11,14,15,20,33]. In order to investigate if this normalization is valid in the specific case, experiments were conducted with another pulse. Specifically, using the function synthesizer mentioned earlier, pulses of 50 kHz were excited. This way the major wavelength was almost 50 mm, resulting in a similar penetration depth. The results of this investigation are presented in Fig. 3(b). Concerning the experiment, the amplitude for the slots up to 9.5 mm was higher than the corresponding of 115 kHz excitation. This is reasonable since the penetration depth of 50 kHz is larger than 115 kHz (wavelengths of 48 mm and 21 mm respectively) and therefore,

more energy propagates under the slot. It is seen that the wavelength of 48 mm is very sensitive even to a small slot of 2 mm. This suggests that lower frequencies, while increasing the penetration depth, can still be used for very shallow defects of concrete. The amplitude showed an almost linear decrease up to the slot of 13.5 mm. Different slots up to this range, resulted in clearly lower amplitude (with the exception of one point) and can be easily characterized. However, this trend was not followed for longer slots, for which the Rayleigh amplitude did not exhibit the same sensitivity, being almost constant for slots larger than 13.5 mm. The numerical results on the other hand, exhibited a smoother decreasing rate for small slots converging to the experimental values for the larger slots simulated.

4.3 Discussion

Figs. 3(a) and (b) show the reduction of the amplitude for the different slots. However, in many similar cases the slot depth values are divided by the wavelength. This is done in order to give a more general form which is applicable in any similar situation but different scale. For example, the reduction in amplitude of a wavelength of 10 mm propagating over a crack of 5 mm, is generally considered similar with the reduction of a wavelength of 100 mm propagating over a crack of 50 mm. Therefore, this normalization makes the relationship more general and applicable to different scale while it is also used in many studies of similar problems [1, 11, 13-15, 17, 18, 20]. In the case of 115 kHz, the slot depths are divided by the major wavelength, λ, of 21 mm, while for 50 kHz they are divided by 48 mm.

The results are presented in Fig. 4. As expected, both the numerical curves follow the same sigmoid trend and the data can easily be grouped into one single master curve. For the largest

slot of 23 mm (larger than the wavelength of 115 kHz), the amplitude is almost zero, being in accordance with the assumption that the major part of Rayleigh energy is distributed within the depth of one wavelength.

The experimental results do not show exactly the same trend for different excitation frequencies. The amplitude for both cases of 115 kHz and 50 kHz, seems to lose its sensitivity to the slot depth for d/λ higher than 0.3, after which the curves are almost horizontal. There can be different reasons for this behavior. One concerns the actual penetration depth of the Rayleigh wave. As mentioned earlier, this is considered to be one wavelength. For ideal non-attenuative material with mechanical properties similar to concrete, it can be calculated that at the depth of one wavelength the amplitude of Rayleigh is 6% of the surface amplitude [8]. However, the attenuation of concrete certainly has an effect decreasing the penetration depth, something that is not accounted for in the numerical solution. Apart from that, the energy of the wave is not proportional to the amplitude but to the square of the amplitude. This implies that the major energy of Rayleigh propagates in a shallower zone. Therefore, despite the fact that the wavelength can be larger than the crack, still the energy passing below the crack is insignificant and therefore, the waveform readings for the larger cracks do not show any discrepancy. Another possible reason for convergence of experimental amplitude to a level higher than zero is the contribution of the longitudinal reflection from the opposite side of the specimen. After the excitation, the major part of energy propagates in the form of Rayleigh on the surface. However, a longitudinal wave is also radiated into the thickness of the specimen. Therefore, it is reasonable to expect a reflection from the opposite side at 150mm. This reflection provides a certain level of energy to the recorded waveform no matter how deep the slot is.

In any case, the amplitude of Rayleigh waves does not exhibit constant sensitivity for all the ranges of crack depths. Concerning metals, it has been stated that the best sensitivity is exhibited in a range where the slot depth is approximately 33% to 66% of the wavelength [24]. In the case of our investigation, the sensitivity is high from very small depths up to about 30% of the Rayleigh wavelength (see Fig. 4), while for larger slots the amplitude remains approximately constant.

It is mentioned that the thickness of the prism specimens did not allow the application of even lower frequencies. For the case of 50 kHz the wavelength is 48 mm. However, Rayleigh waves do not form at depths larger than half the beam depth [13] and therefore, the use of longer wavelengths would be problematic.

It is interesting to observe the frequency content of the pulse. As mentioned, the major peak using the first configuration is at 115 kHz. This is depicted in Fig. 5 for the sound material case. This frequency corresponds to a wavelength of 21 mm. Therefore, according to the theoretical assumption that the energy propagates up to one wavelength in depth, it would be expected that no or almost no energy in the band of 115 kHz survives past the crack of 23 mm. However, as seen in Fig. 5, the peak of 115 kHz still contains the main part of the pulse energy. This should be due to the back side reflection or the crack tip refraction. The low frequency peak does not seem very much influenced though, since it corresponds to a wavelength of 60 mm and sufficient energy passes also below the crack.

4.4 Complete repair of the slot

A typical treatment of surface cracks is application of epoxy agent that seals the openings and protects the interior from environmental influence, offering also improvement of structural strength [1,7,8]. Two of the cracks were totally filled with epoxy. In Fig. 6(a) the waveform collected at the slot of 13.5 mm after epoxy injection can be compared to the one obtained before the application of epoxy (empty slot), as well as to the sound material response. It is seen that the injection of epoxy, greatly enhances wave propagation, increasing the transmitted energy to almost the levels of the sound material. Accordingly, the Rayleigh wave is restored and the characteristic strong negative peak can be identified, although it is observed 3 μs later than the case of sound material. Based on this point, the velocity is calculated to the value of 2051 m/s while in the sound concrete it was measured at 2440 m/s. This drop is reasonable due to the epoxy layer that has certainly lower elastic modulus, i.e. 1 GPa. However, the epoxy layer is too thin to be responsible for the whole velocity decrease. A possible other reason, as has been stated in a number of cases [8,34] is the existence of the fracture process zone, a zone of deteriorated concrete at both sides of the crack. It is mentioned that in the frequency domain the energy was increased similarly to the time domain, without however, any specific peak or band being more characteristic. The above investigation shows that surface measurements supply the possibility to characterize the efficiency of repair.

The numerical results for the case of fully repaired crack are presented in Fig. 6(b). It is seen that the case of fully filled slot, exhibits almost as high amplitude as the sound material, specifically 91% of the sound concrete. This shows that the narrow layer of epoxy, although

has elasticity several times lower than concrete, greatly enhances the propagation through the crack, while it almost restores the amplitude to the initial level.

The above experimental and numerical results reveal a very important trend for in-situ application. If the repair is successful, and the epoxy filling of the crack is complete, the amplitude of the surface wave should compare to the reference measurement on sound material. On the other hand, if the amplitude is not high, this implies shortage of repair agent in the crack volume.

4.5 Partial repair of the slot

A case of interest is the partially grouted cracks. In many cases a large part of the crack remains unfilled, especially if the injection is not conducted with an adequate pressure. However, since the space near the mouth of the crack is filled with grout/epoxy, this permits the propagation of stress waves resulting in difficulty to obtain information about the extent of grouting by transit time or amplitude data [9]. To study this case, some slots were partially filled with epoxy. A thick piece of hard paper was wrapped in a Teflon sheet and placed inside the slot leaving an empty space on top. This space was filled with epoxy. Then, the paper was removed by pulling from one side leaving only the epoxy layer on the top part of the slot, as seen in the cross section of Fig. 7.

The cases examined, concern filling of 2 mm and 9 mm to the slot of 19 mm and filling of 3 mm and 11 mm to the slot of 23 mm. Therefore, the filling ranges from about 10% to 50%. Stress wave measurements were conducted using the configuration with the broad-band

sensors and the PAC pulser of 115 kHz main excitation. The amplitude results are presented in Fig. 8(a). It is seen that the slight filling near the mouth of the crack substantially increases the amplitude. This increase should be attributed to the Rayleigh wave but also to the longitudinal and shear arrivals that pass through the epoxy layer. For filling up to about 50% of the crack, the amplitude is restored to more than 50% of the sound material. This curve shows that the amplitude can characterize the repair since it increases clearly and monotonically with the filling.

In Fig. 8(b) numerical results are presented for the cases of three different slots with filling of 1/3 and 2/3 of their depth. The curves, although translated to lower values compared to the experimental, show a similar sigmoid trend with a higher increase rate for low filling percentage and small amplitude difference for 33% and 67% of filling.

The above results can be characterized indicative, but they show the potential for more accurate characterization in case they are further studied and more slot cases, as well as filling contents are examined.

It is mentioned that the purpose was to simulate as close as possible the actual crack situation. Therefore, the numerical computations were derived for crack mouth opening of 0.5 mm, which is close to actual cracks observed in concrete [8]. However, in order to check the effect of crack width, some simulations for empty slots were repeated for opening of 4 mm, similar to the slots used for the experimental part. The waveforms showed that the effect of slot width is not important at least for the scale applied, see Fig. 9

5. In situ application

Generally, it can be argued that coupling conditions or other difficult to control circumstances, can affect the measurements in situ. The roughness of the surface, or the coupling agent used, can influence the readings and should be responsible for an amount of experimental scatter. However, it seems that the epoxy filling of a crack provides an increase of transmission much higher than any possible fluctuation due to random effects. This is discussed in the example below.

Surface cracks were observed on a concrete bridge deck. The cracks were through the thickness of the whole deck and therefore, there was no need for depth estimation. The wave monitoring aimed at the evaluation of the repair that was conducted using epoxy injection. Details about the whole monitoring project can be found in [8]. For the ultrasonic examination, an array of five receivers was used with a separation distance of 50 mm while the crack was between the 3rd and the 4th. The excitation was conducted by pencil lead break, providing a bandwidth up to 200 kHz. In Fig. 10(a), the recorded waveforms of the sensors for the case of open crack are depicted. It is seen that after the initial longitudinal arrivals, a strong Rayleigh burst is observed for the first 3 transducers, at 0 mm, 50 mm and 100 mm from the excitation. However, after the crack, the energy of the waveform is minimized, and certainly no Rayleigh pattern is identified for the distances of 150 mm and 200 mm, similarly to another case described in [8].

In Fig. 10(b) one can see the waveforms after application of epoxy. It is seen that the energy of the 4th and 5th waveforms was greatly enhanced and a Rayleigh peak was identified as

indicated by the circles in Fig. 10(b). The Rayleigh velocity measured was 10% lower than the sound concrete, something that can be attributed to the fracture process zone.

In this case, since the Rayleigh wave was restored, the surface portion was substantially filled. It is noted that according to the frequency and the Rayleigh velocity, the wavelength is calculated at 35-40mm.

6. Conclusion

In the present paper, the problem of wave propagation through surface opening cracks is dealt with, both experimentally and numerically. The study is focused on the amplitude of the Rayleigh wave and its dependence on the crack depth. Experimental and numerical results show good qualitative agreement concerning both the amplitude vs. empty slot depth relation, as well as the case of fully or partially repaired crack. Filling the empty crack volume with a repairing material, even of inferior mechanical properties, restores the propagation to the level of sound material, as confirmed both by experimental and numerical results. Additionally, the issue of characterization of partial filling is addressed showing good potential, since the epoxy percentage can be correlated to the amplitude of the wave.

Concerning the crack depth determination, although a relationship between amplitude and crack depth is suggested, based on one single curve (like the ones of Fig. 4) it would be difficult to characterize accurately any slot, except for the smallest ones with depth to wavelength less than 0.3. Therefore, a multivariate approach seems more appropriate. It is

mentioned that apart from the amplitude, different parameters can be studied. These, could be the total energy of the pulse, the waveform peak time [22] the time centroid and the accumulated amplitude of the rectified waveform [4,27], as well as the cut off frequency [20].

An interesting future task would be the experimental investigation at larger concrete blocks, with deeper slots that simulate closer the actual defects at concrete sites. In any case, using only the amplitude of Rayleigh waves can still provide valuable information concerning the efficiency of repair, as indicated by the example of in-situ application described herein.

References

[1] Hevin G, Abraham O, Pedersen HA, Campillo M. Characterisation of surface cracks with Rayleigh waves: a numerical model. NDT&E International 1998;31(4):289-297.

[2] Issa CA, Debs P. Experimental study of epoxy repairing of cracks in concrete. Construction and Building Materials 2007;21:157-163.

[3] Ono K. Damaged concrete structures in Japan due to alkali silica reaction. The International Journal of Cement Composites and Lightweight Concrete 1988;10(4):247-257.

[4] Kruger M. Scanning impact-echo techniques for crack depth determination. Otto-Graf-Journal 2005;16:245-257.

[5] Shiotani T, Nakanishi Y, Iwaki K, Luo X, Haya H. Evaluation of reinforcement in damaged railway concrete piers by means of acoustic emission. Journal of Acoustic Emission 2005;23:260-271.

[6] Binda L, Modena C, Baronio G, Abbaneo S. Repair and investigation techniques for stone masonry walls. Construction and Building Materials 1997;11(3):133-142.

[7] Thanoon WA, Jaafar MS, Razali M, Kadir A, Noorzaei J. Repair and structural performance of initially cracked reinforced concrete slabs. Construction and Building Materials 2005;19(8):595-603.

[8] Aggelis DG, Shiotani T. Repair evaluation of concrete cracks using surface and through-transmission wave measurements, Cement and Concrete Composites 2007;29:700-711.

[9] Sansalone MJ, Streett WB. Impact-echo nondestructive evaluation of concrete and masonry. Ithaca, N.Y: Bullbrier Press; 1997.

[10] Naik TR, Malhotra VM. The ultrasonic pulse velocity, in: Malhotra VM, Carino NJ (Eds.). CRC Handbook on Nondestructive Testing of Concrete, Florida, CRC Press, 1991, 169-188.

[11] Tsutsumi T, Wu J, Wu J, Huang X, Wu Z. Introduction to a new surface-wave based NDT method for crack detection and its application in large dam monitoring. Proc. Int. Symposium on Dam Safety and Detection of Hidden Troubles of Dams and Dikes, 1-3 November 2005, Xian China (CD-ROM).

[12] Liu PL, Lee KH, Wu TT, Kuo MK. Scan of surface-opening cracks in reinforced concrete using transient elastic waves. NDT&E INT 2001;34:219-226.

[13] Zerwer A, Polak MA, Santamarina JC. Detection of surface breaking cracks in concrete members using Rayleigh waves. Journal of Environmental and Engineering Geophysics 2005;10(3):295-306.

[14] Pecorari C. Rayleigh wave dispersion due to a distribution of semi-elliptical surface-breaking cracks. Journal of the Acoustical Society of America 1998;103(3):1383-1387.

[15] Pecorari C. Scattering of a Rayleigh wave by a surface-breaking crack with faces in partial contact. Wave Motion 2001;33:259-270.

[16] Graff KF. Wave motion in elastic solids. New York: Dover Publications; 1975.

[17] Doyle PA, Scala CM. Crack depth measurement by ultrasonics: a review. Ultrasonics 1978;16(4):164-170.

[18] Achenbach JD, Cheng A. Depth determination of surface-breaking cracks in concrete slabs using a self-compensating ultrasonic technique. Review of Progress in Quantitative Nondestructive Evaluation; Vol. 15B, DO Thompson and DD Chimenti

(eds), Plenum Press, New York and London, 1996(1763-1770).

[19] Arias I, Achenbach JD. A model for the ultrasonic detection of surface-breaking cracks by the scanning laser source technique. Wave Motion 2004;39(1):61-75.

[20] Edwards RS, Dixon S, Jian X. Depth gauging of defects using low frequency wideband Rayleigh waves. Ultrasonics 2006;44:93-98.

[21] Song WJ, Popovics JS, Aldrin JC, Shah SP. Measurements of surface wave transmission coefficient across surface-breaking cracks and notches in concrete. Journal of the Acoustical Society of America 2003;113(2):717-725.

[22] Ramamoorthy SK, Kane Y, Turner JA. Ultrasound diffusion for crack depth determination in concrete. Journal of the Acoustical Society of America 2004;115(2):523-529.

[23] Zhang C, Achenbach JP, Dispersion and attenuation of surface waves due to distributed surface-breaking cracks. J. Acoust. Soc. Am. 1990;88(4):1986-1992.

[24] Yew CH, Chen KG, Wang DL. An experimental study of reflection between surface waves and a surface breaking crack. J. Acoust. Soc. Am. 1984;75(1):189-196.

[25] Masserey B, Mazza E. Analysis of the near-field ultrasonic scattering at a surface crack. J. Acoust. Soc. Am. 2005;118(6): 3585-3594.

[26] Masserey B, Mazza E. Ultrasonic sizing of short surface cracks. Ultrasonics 2007;46:195-204.

[27] Shiotani T, Aggelis DG. Determination of surface crack depth and repair effectiveness using Rayleigh waves. Fracture Mechanics of Concrete and Concrete Structures – Design, Assessment and Retrofitting of RC Structures – Carpinteri A., Gambarova P., Ferro G., Plizzari G., (eds.), UK, London: Taylor & Francis, 2007 (pp. 1011-1018).

[28] Polyzos D, Tsinopoulos SV, Beskos DE, Static and Dynamic Boundary Element Analysis in Incompressible Linear Elasticity. European Journal of Mechanics A/Solids 1998;17(3):515-536.

[29] Kausel E, Röesset JM. Frequency domain analysis of undamped systems. Journal of Engineering Mechanics ASCE 1992;118:721–734.

[30] Kattis SE, Polyzos D, Beskos DE. Vibration Isolation by a Row of Piles Using a 3-D Frequency Domain BEM. International Journal of Numerical Methods in Engineering 1999;46:713-728.

[31] Guiggiani M and Casalini P. Direct computation of Cauchy principal value integrals in advanced boundary elements. International Journal for Numerical Methods in Engineering 1987;24:1711–1720.

[32] Qixian L, Bungey JH. Using compression wave ultrasonic transducers to measure the velocity of surface waves and hence determine dynamic modulus of elasticity for concrete. Construction and Building Materials 1996;10(4):237-242.

[33] Toutanji H. Ultrasonic wave velocity signal interpretation of simulated concrete bridge decks. Materials and Structures 2000;33:207-215.

[34] Mihashi H, Nomura N, Niiseki S. Influence of aggregate size on fracture process zone of concrete detected with three dimensional acoustic emission technique. Cement and Concrete Research 1991;21:737-744.

Figure captions

Fig. 1 Geometry of the experiment.

Fig. 2 Waveforms collected after different slots, using excitation of 115 kHz (a) experimental, (b) numerical.

Fig. 3 Amplitude vs. slot depth relationship using (a) 115 kHz and (b) 50 kHz.

Fig. 4 Amplitude vs. slot depth/wavelength relationship.

Fig. 5 Fast Fourier transform of different signals.

Fig. 6 Waveforms collected for different conditions of concrete (a) experimental, (b) numerical.

Fig. 7 Schematic representation of partially epoxy filled slot.

Fig. 8 Amplitude vs. epoxy filling percentage of different slots, (a) experimental, (b) numerical. (The curves connect the symbols in order to indicate the increasing trend and are not results of curve fitting).

Fig. 9 Waveforms of 115 kHz collected after 9.5 mm deep slot for different slot width.

Fig. 10 Waveforms collected at different distances from the excitation on the bridge deck (a) before and (b) after repair with epoxy injection. The crack is at the position of 125 mm.

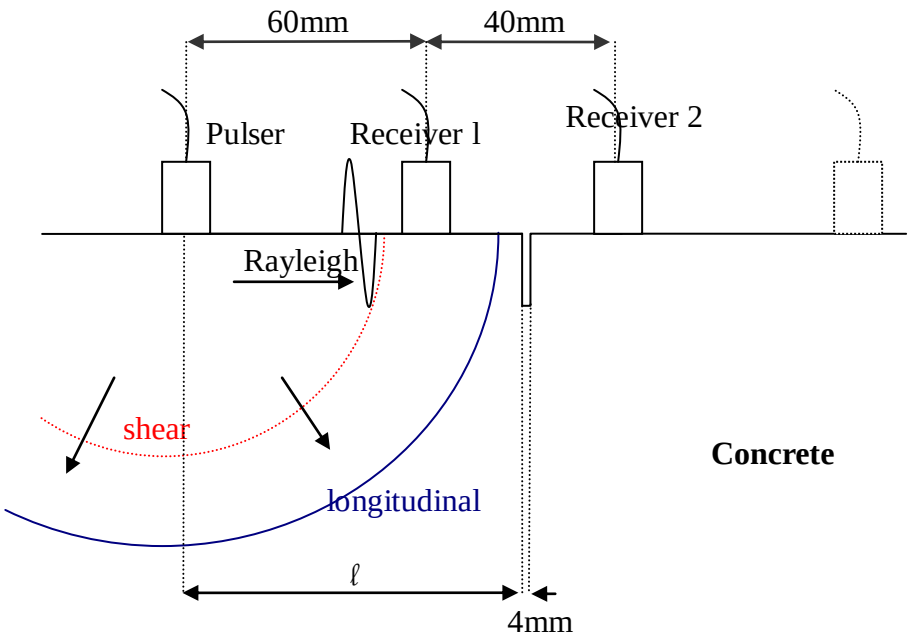

Fig. 1 Geometry of the experiment.

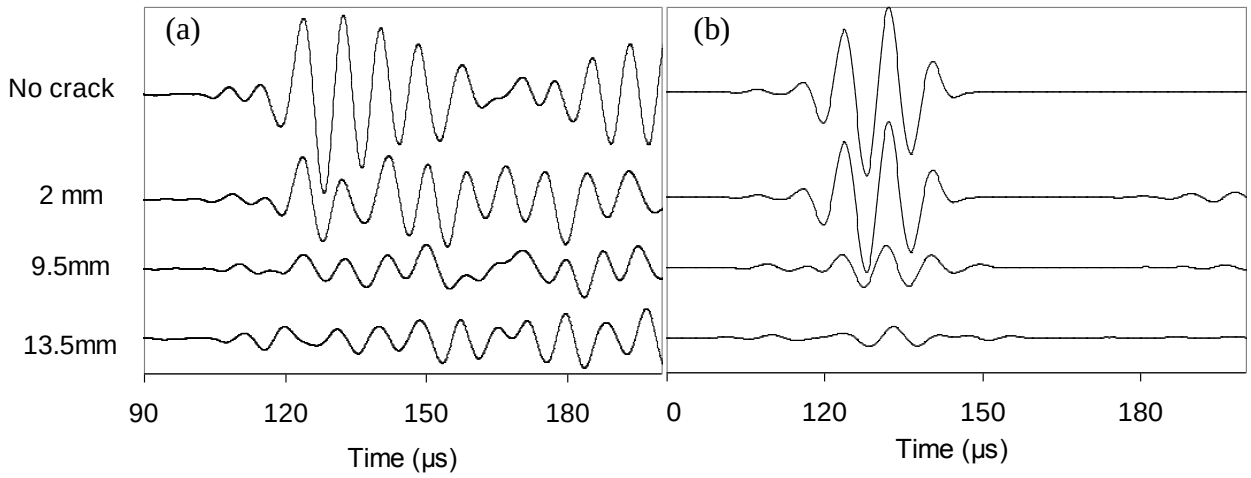

Fig. 2 Waveforms collected after different slots, using excitation of 115 kHz (a) experimental, (b) numerical.

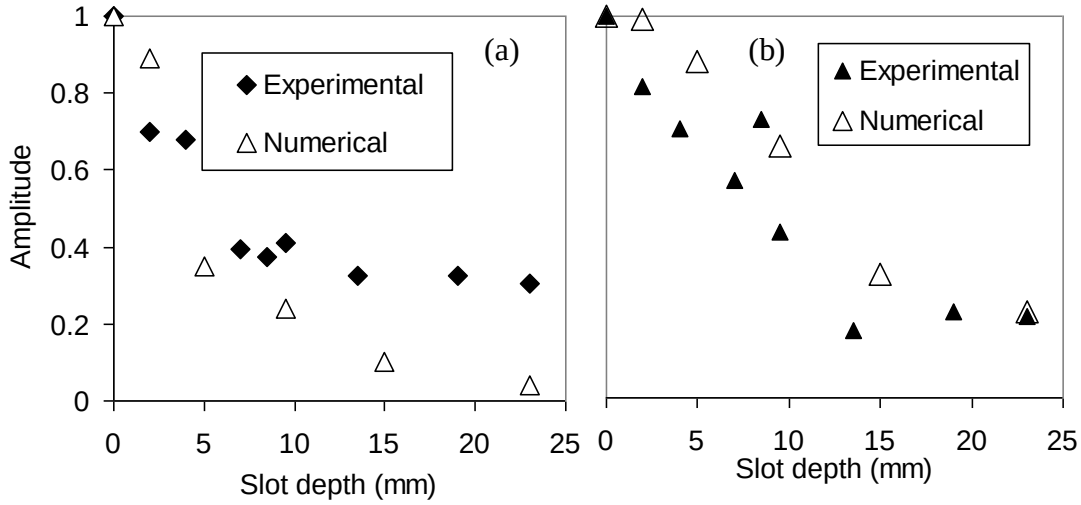

Fig. 3 Amplitude vs. slot depth relationship using (a) 115 kHz and (b) 50 kHz.

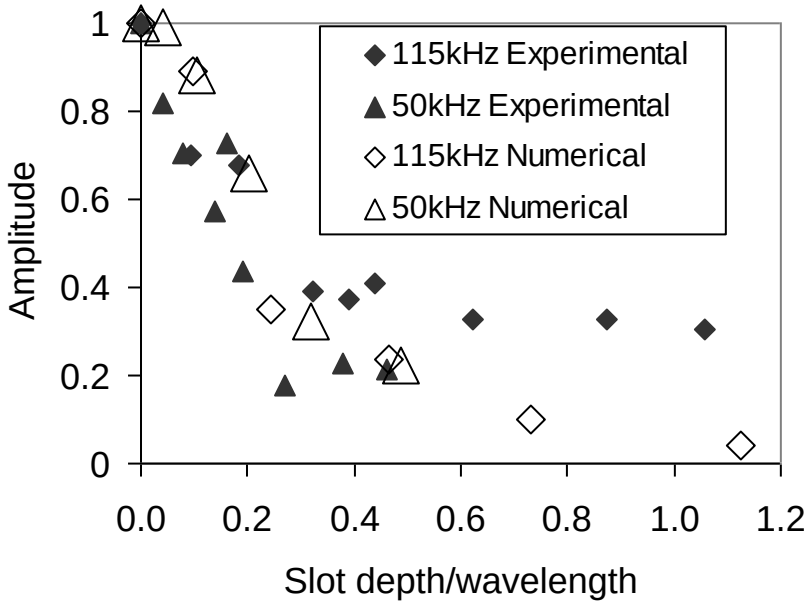

Fig. 4 Amplitude vs. slot depth/wavelength relationship.

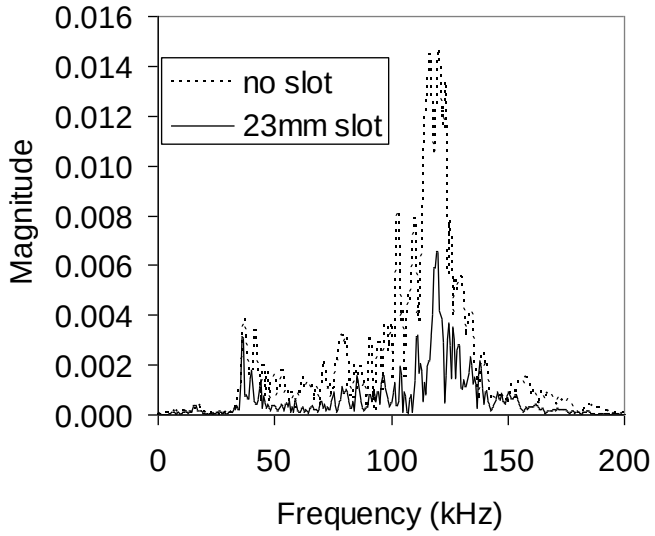

Fig. 5 Fast Fourier transform of different signals.

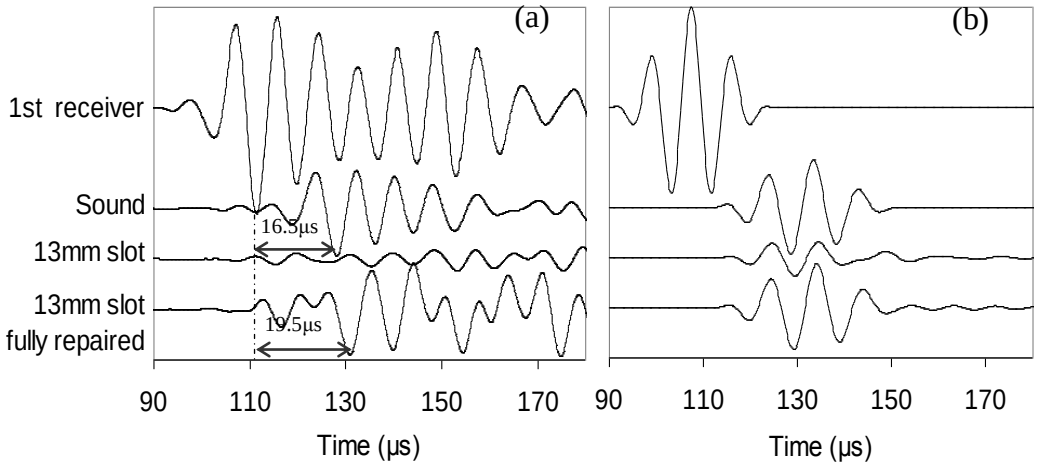

Fig. 6 Waveforms collected for different conditions of concrete (a) experimental, (b) numerical.

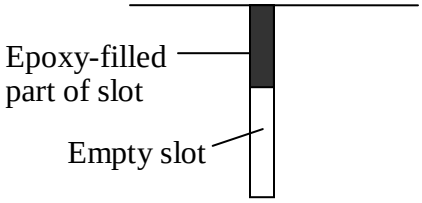

Fig. 7 Schematic representation of partially epoxy filled slot.

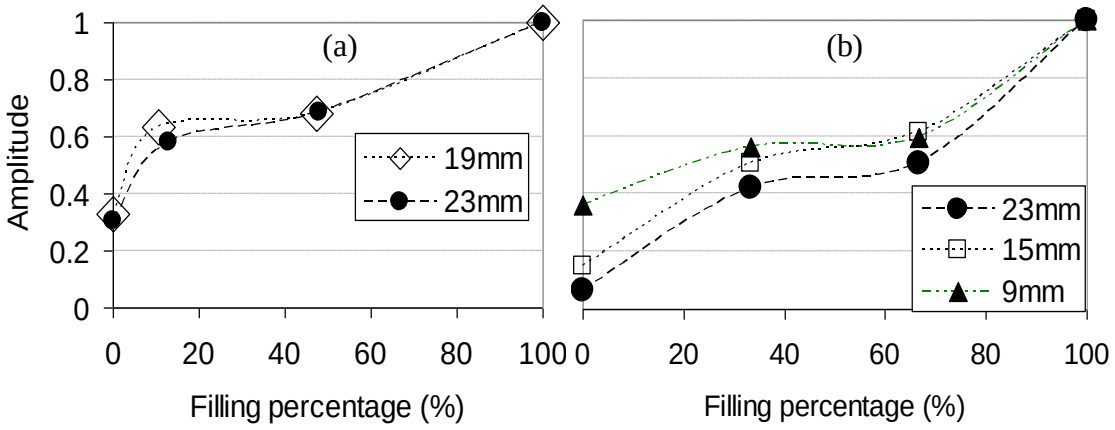

Fig. 8 Amplitude vs. epoxy filling percentage of different slots, (a) experimental, (b) numerical (The curves connect the symbols in order to indicate the increasing trend and are not results of curve fitting).

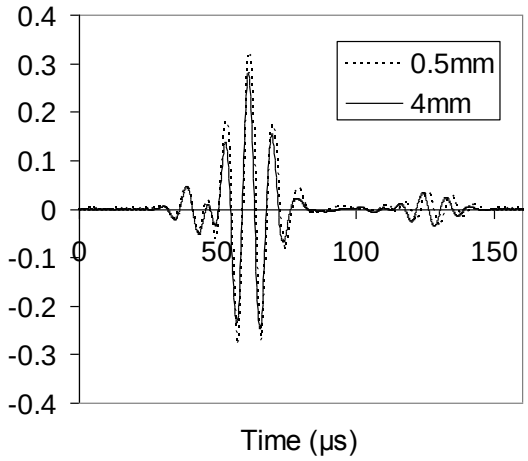

Fig. 9 Waveforms of 115 kHz collected after 9.5 mm deep slot for different slot width.

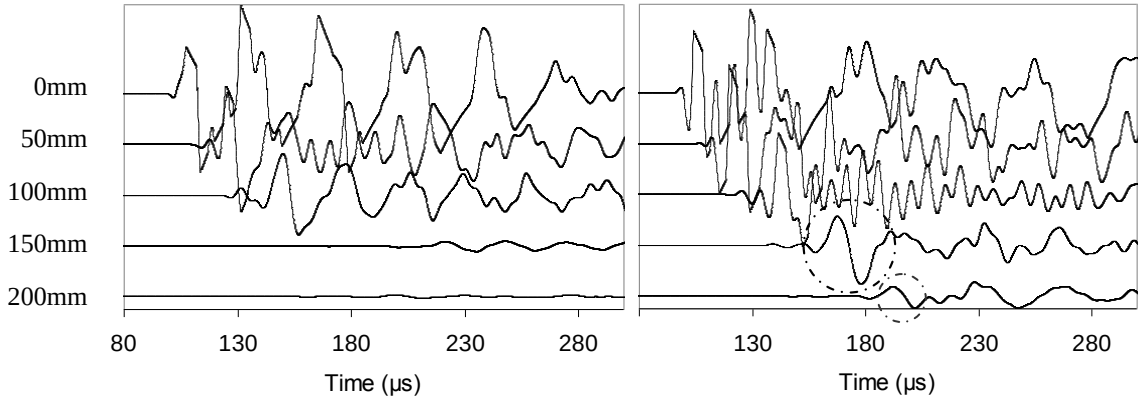

Fig. 10 Waveforms collected at different distances from the excitation on the bridge deck (a) before and (b) after repair with epoxy injection. The crack is at the position of 125mm.